

Computational Fluid Dynamics Analysis of Blood Flow in Human Aorta

Yogesh V. Borse¹, Prof. S.A. Giri²

M. Tech Scholar, Dept of Mechanical Engg, Ramdeobaba College of Engineering and Management, Nagpur, India¹

Assistant Professor, Dept of Mechanical Engg, Ramdeobaba College of Engineering and Management, Nagpur, India²

Abstract: Computational fluid dynamics becomes a powerful tool to gain insight into the physical behaviour of the cardiovascular system. An area of cardiovascular disease has received little attention from a computational viewpoint is the analysis of arterial stiffening with age and disease and its relationship with the underlying blood flow behaviour. Due to the complex geometry and material properties of the Aorta, therein, large-scale three dimensional computational models of arterial mechanics can improve our ability to interpret current clinical hemodynamic metrics and to advance our fundamental understanding of the mechanisms of disease progression. In the present research, three dimensional geometry of Aorta is created in CATIA and blood flow behaviour is analysed by Ansys CFX. Mainly, pulsatile flow is investigated for 10 timesteps, Blood is modeled as Newtonian fluid, and the viscous laminar model is employed for the analysis. The CFD simulations successfully produce the effect of blood pressure on the structure of human Aorta; this demonstrated that the methodology can be used to explore blood flow behaviour in Aorta and to relate these to important clinical issues.

Keywords: computational fluid dynamics (CFD), Aorta, Ansys CFX

I. INTRODUCTION

Atherosclerosis begins with the accumulation of low-density lipoprotein under the endothelial layer and the contribution of neutrophils and smooth muscle cells. As the lesion progresses^[1], these cells become filled with lipids, a raised area of intima appears, and a thick, fibrous plaque is gradually formed. Over time, these plaques may narrow the arterial lumen and obstruct the blood flow. Often, a plaque will rupture suddenly, creating an acute obstruction to blood flow. Ischemic heart disease, the most fatal form of CVD, results from obstruction of blood flow to the heart and is usually caused by atherosclerotic plaques in the coronary arteries. The seven leading causes of death of women over age 18 in the United States are^[2] heart disease, cancer, stroke, chronic lower respiratory disease, Alzheimer's disease, unintentional injuries, and diabetes mellitus. Based, heart disease and cancer are the first and second leading causes of death for African-American, White, and Hispanic women in the U.S. However, for American-Indian/Alaska-Native and Asian- or Pacific-Islander women, cancer is the leading cause of death and heart disease is the second leading cause of death. Stroke is the third leading cause of death for all women except for American-Indian/Alaska-Native women.

The aorta is a large artery that branches into many smaller arteries, arterioles, and ultimately capillaries. In the capillaries, oxygen and nutrients from the blood supply to body cells for metabolism, and exchanged for carbon dioxide and waste products. The aorta is an elastic artery, and as such is quite distensible. The aorta consists of a heterogeneous mixture of smooth muscle, nerves, intimal cells, endothelial cells, fibroblast-like cells, and a complex extracellular matrix. The vascular wall consists of several

layers known as the tunica externa, tunica media, and tunica intima. The thickness of the aorta requires an extensive network of tiny blood vessels called vasa vasorum, which feed the tunica externa and tunica media outer layers of the aorta. The aortic arch contains baroreceptors and chemoreceptors that relay information concerning blood pressure and blood pH and carbon dioxide levels to the medulla oblongata of the brain. This information is processed by the brain and the autonomic nervous system mediates the homeostatic responses.

II. RELATED WORK

There have been many researches associated to this area. Larissa Huetter, et al Larissa Huetter, et al. (2015) could yield^[3] important information to guide further research into the hemodynamic therapy for critically ill patients, predict the performance of surrogate heart valves in silico, or model the outcomes of coronary artery disease. By ensuring that the geometry of the aorta phantom is as close as possible to realistic conditions which can be used for the further analysis, Mona Alimohmmadi, Joseph et.al^[4] Patient-specific anatomical details were extracted from computed tomography images two way FSI Simulation were performed with coupled boundary conditions & hyperelastic wall properties. FSI methodology employed was appropriate for simulations of aortic dissection. Regions of high wall shear stress were not significantly altered by the wall motion, however certain collocated regions of low & oscillatory wall shear stress which may be critical for disease progression were only identified in FSI simulation. M. Malvè, et.al^[5] proposed a Fluid Solid Interaction analysis (FSI) of a computerized tomography (CT) scan reconstructed left coronary artery was

performed. The arterial wall was modeled as an isotropic hyperelastic material. The arterial wall shear stress (WSS) was computed in order to investigate a correlation between flow induced wall shear stress and geometry of the artery. An unsteady state FSI analysis with commercial finite element software was performed in order to evaluate the maximum and the minimum wall shear stress as a function of the flow regime and the arterial wall compliance in the left coronary. As boundary conditions, physiological pressure waveforms were applied. Comparison of the computational results between the FSI and rigid-wall models showed that the wall shear stress (WSS) distributions were substantially affected by the arterial wall compliance. In particular, the minimum and maximum WSS values significantly vary. M.Alishahi, et.al studied [6] the two different geometry of healthy & severely stenosed abdominal aorta, extracted from CT scan images & simulations of fluid flow & tissue interaction (Fluid solid Interaction) are carried out. Computed Pressure is lower by 15% for flexible model, as compared to the rigid. Tina M. Morrison, Phd reported that [7] the longitudinal and circumferential biomechanical cyclic strain in younger and older patients with no visible signs of aortic pathology, along with length and diameter changes in the as well as diameter changes along the thoracic aorta. The aorta enlarges circumferentially and axially, and deforms significantly less in the circumferential and longitudinal directions. This analysis is a first step in understanding and quantifying the cyclic strains of the thoracic aorta, and creating a foundation for standards in reporting data related to in vivo deformation. Changes in thoracic aorta cyclic strains were quantified using cardiac-gated computed tomography image data of 14 patients (aged 35 to 80 years) with no visible aortic pathology (aneurysms or dissection). We measured the diameter and circumferential cyclic strain in the arch and descending thoracic aorta (DTA), the longitudinal cyclic strain along the DTA, and changes in arch length and motion of the ascending aorta relative to the DTA. Diameters were computed distal to the left coronary artery, proximal and distal to the brachiocephalic trunk, and distal to the left common carotid, left Subclavian, and the first and seventh intercostal arteries. Cyclic strains were computed using the Green-Lagrange strain tensor. Arch length was defined along the vessel centerline from the left coronary artery to the first intercostal artery. The length of the DTA was defined along the vessel centerline from the first to seventh intercostal artery. Longitudinal cyclic strain was quantified as the difference between the systolic and diastolic DTA lengths divided by the diastolic DTA length Comparisons were made between seven younger (age, 41 _ 7 years; 5 men) and seven older (age, 68 _ 6 years; 5 men) patients. The average increase of diameters of the thoracic aorta was 14% with age from the younger to the older (mean age, 41 vs. 68 years) group. The average circumferential cyclic strain of the thoracic aorta decreased by 55% with age from the younger to the older group. The longitudinal cyclic strain decreased with age by 50% from the younger to older group .The arch length increased by 14% with age from the younger to the older group.

III.CASE DESCRIPTION

The simulation were based on Aorta of younger person [7], Fig 1 shows the complete CFD simulation process. Following are the steps in CFD simulation.

A. Geometric Model and Material Properties

The geometry of the aortic arch depends on gender, age, central blood pressure and hemodynamic health of the individual [8]. Therefore, a further step in this research was to consider the geometry of individuals that have hemodynamic dysfunction.

To do this, access to an MRI or CT data from the critically ill individuals to build a physiologically realistic model was required. The critically ill patient specific flow field could then be compared to the idealized one to measure the validity of some of the assumptions regarding hemodynamic dysfunction

3D geometrical model of younger person was composed of curves and surfaces were created in CATIA V5, based on the dimensions in TABLE 1 and Fig.2 which was a simpler tool for geometry creation than Ansys. The geometry was created in two domains one was the structural domain (Aorta wall) and another was a fluid domain (Blood) as shown in Fig.3. The density of Aorta wall was set to 1120kg/m³. Young's modulus and Poisson's ratio of the Aorta wall were set to 1.08 MPa and 0.49, respectively [9], which are within the physiological range.

TABLE 1

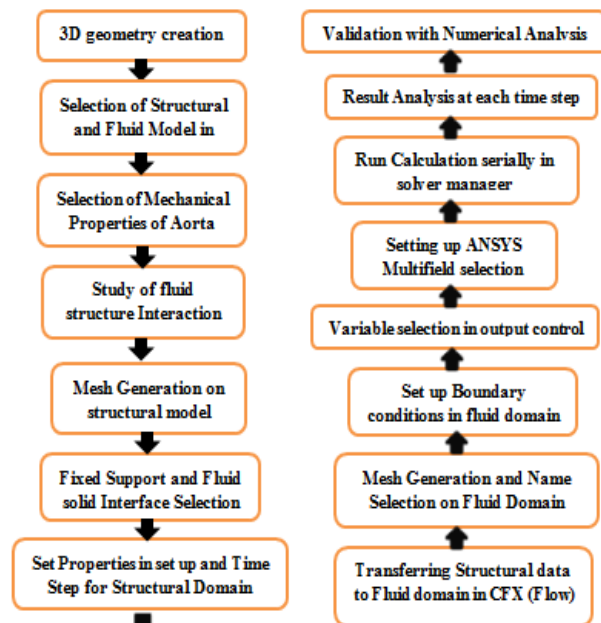


Fig.1 Flow chart of CFD analysis

The diameters and circumferential cyclic strains for the ascending aorta, the arch, and the descending aorta was reported for the younger and older groups [7] a Each

number, 1 to 7, corresponds to the aortic location shown in the figure Values for P were computed between the younger and older group for each location using the paired t test.

Variable, mean ± SD	1	2	3	4	5	6	7
Diameter, mm							
Young	31.9 ± 4.7	31.1 ± 3.9	27.1 ± 1.7	25.2 ± 1.3	23.5 ± 1.1	22.8 ± 1.0	21.1 ± 1.4
Older	32.3 ± 4.3	34.7 ± 2.0	32.4 ± 3.6	29.1 ± 2.6	26.1 ± 2.5	26.6 ± 3.0	24.5 ± 2.8
P ^b	=.56	=.11	<.05	<.01	<.05	<.05	<.05
Cyclic strain, %							
Young	10.3 ± 3.8	11.3 ± 6.9	8.8 ± 3.8	8.9 ± 3.5	7.9 ± 2.4	7.3 ± 2.6	8.1 ± 3.3
Older	2.6 ± 1.2	3.4 ± 1.5	1.6 ± 1.4	2.7 ± 1.4	2.0 ± 2.0	2.7 ± 1.3	4.2 ± 1.9
P ^b	<.01	<.01	<.01	<.01	<.001	<.01	<.01

Schematic of the thoracic aorta where the numbers correspond to location of measurement.

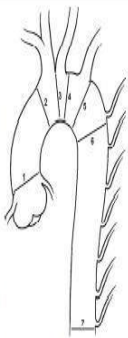
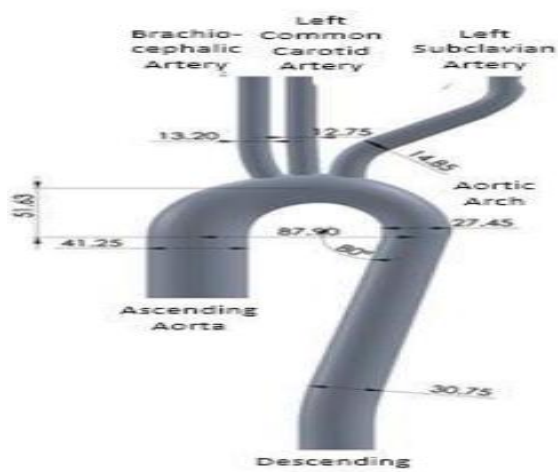



Fig.2 1:1.5 Model of the aorta [3]

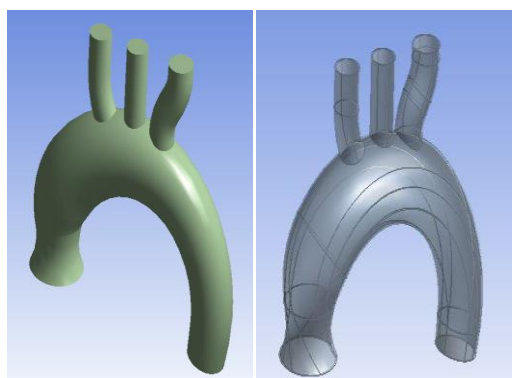
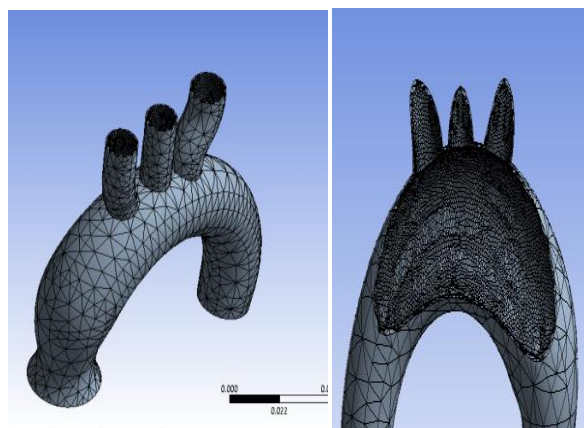


Fig.3 Geometry of the Structural domain (Left) And Fluid domain (Right)

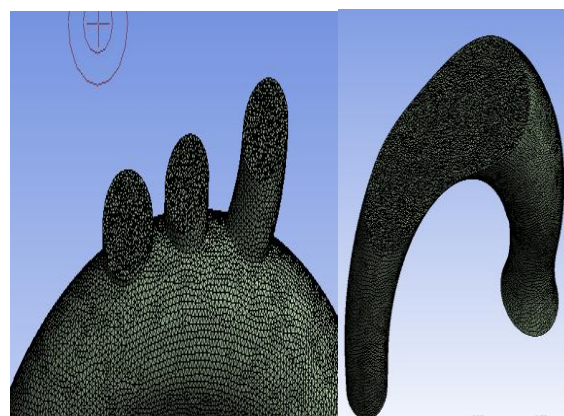
B. Meshing

Fig. 4 shows detailed mesh view of Aorta wall and blood domain, coarse mesh had been selected for the analysis by reducing element size to 1mm, 150476 and 218174 nodes

were generated for Aorta wall and blood domain respectively.



(a)



(b)

Fig. 4 Detailed mesh view of (a) Aorta wall (b) Blood domain

c. Boundary Conditions

Fig.5 shows the selected boundaries for the analysis of blood flow through Aorta, inside surface of Aorta wall was selected as a fluid solid interface to analyse the effect of fluid forces on the Aorta wall. The simulation was performed for unsteady flow analysis and since the geometry was highly complicated and mesh was highly skewed; low time step and coarse mesh of fluid part was to be chosen for better mapping at fluid solid interface region. low time step of 0.083s was selected and the simulation ran for 10 time steps.

Viscous laminar model was to be chosen with Ansys multifield, receives information from total mesh displacement and send it to the total force for better coupling of fluid structure interaction. The FSI simulation in this work was an attempt to simulate the blood flow using Ansys Workbench since it only run for 10 time steps. Global initialization has been required for the unsteady state analysis setting initial velocity at inlet of aorta to 0.098 m/s and pressure inlet to 19065 Pa, velocities at outlet 1, outlet2, outlet3 and outlet were to be selected as 0.45 m/s, 0.4 m/s, 0.4 m/s and 0.6 m/s which are within the blood flow range of normal human.

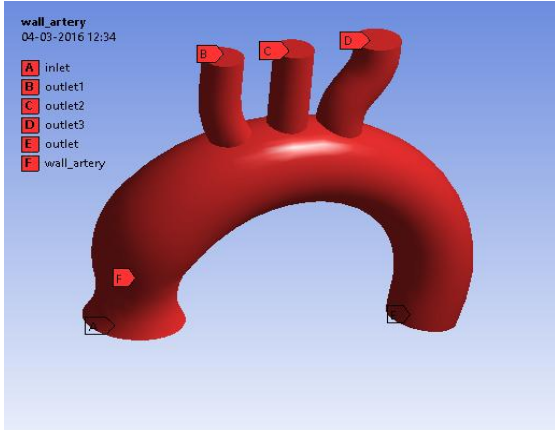
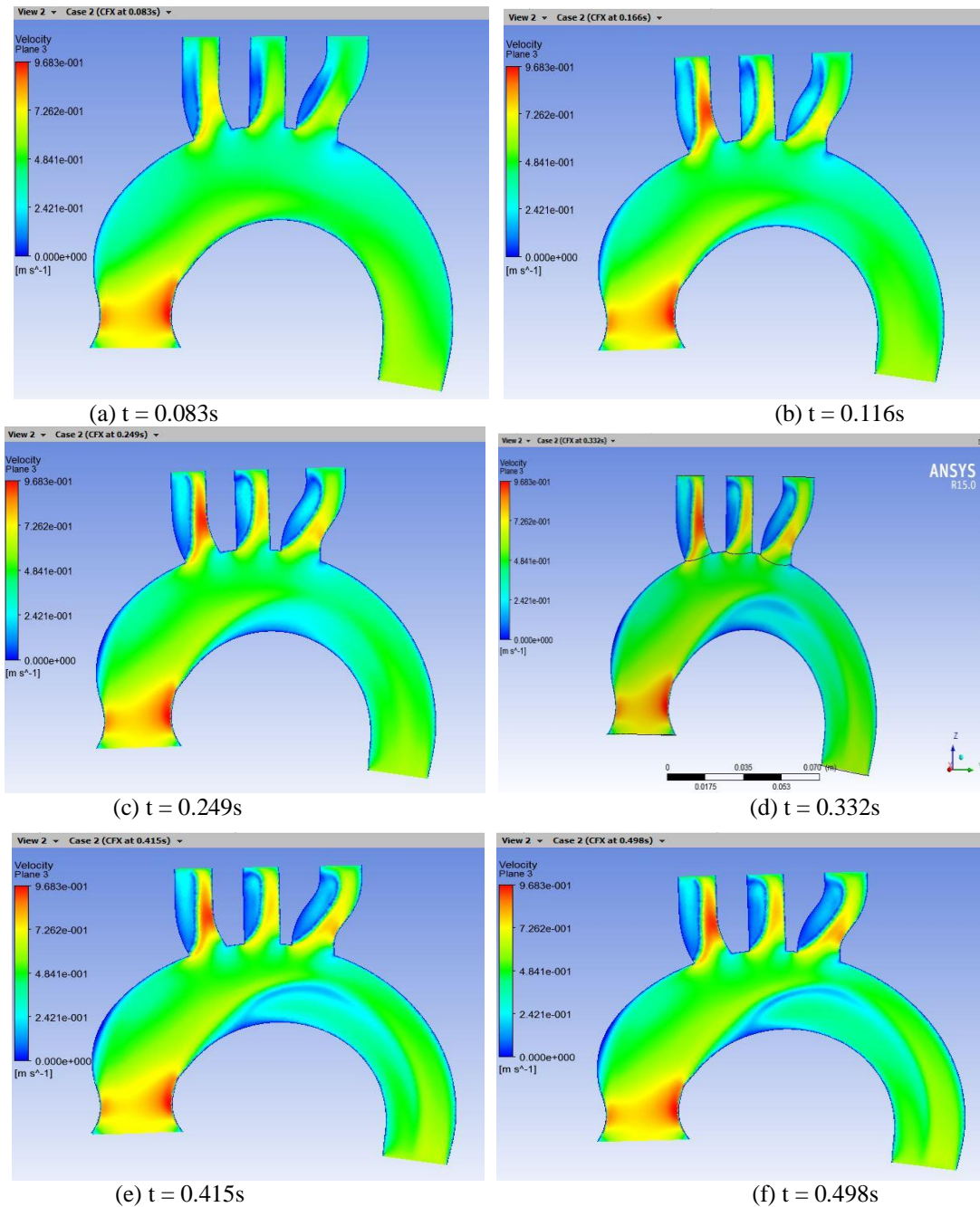


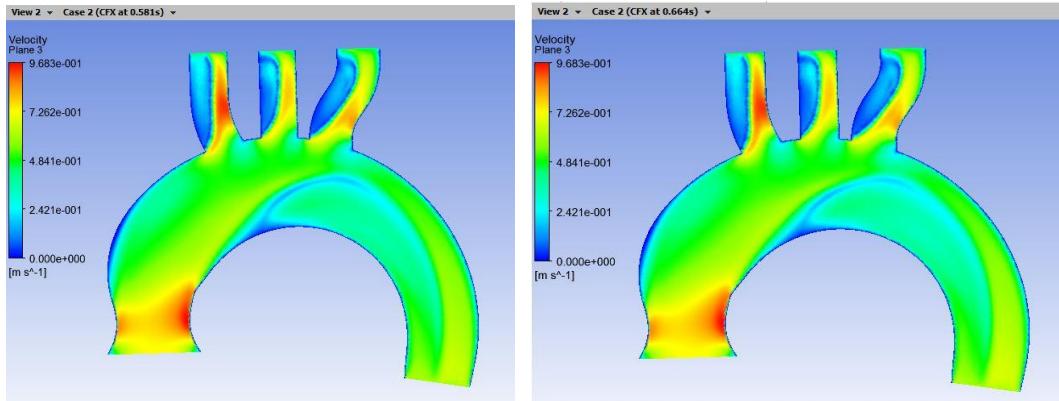
Fig.5 Inlet and Outlet boundary conditions

IV. RESULTS AND DISCUSSION

In fig 6 velocity variations at each time step has been plotted and it is observed that, velocity variation with respect to time is more up to 0.332s and which is less after 0.332s. During the peak flow phase, 0.083, 0.116 and 0.332 seconds, the velocity located near the inner curvature of the aorta is higher than that near the outer curvature. During the flow deceleration phase, 0.415 to 0.83 seconds, flow near the wall becomes skewed, especially along the outer curvature, while the flow in the centre continues in the axial direction. Maximum velocity is observed at the right brachiocephalic artery compare to the left subclavian artery.

1. Velocity Contours

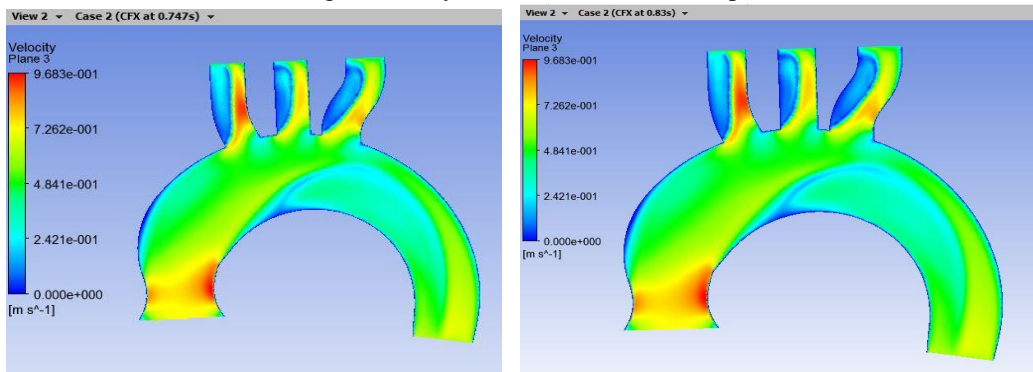




(g) $t = 0.581s$

(h) $t = 0.664s$

Fig.6 Velocity variation at each time step

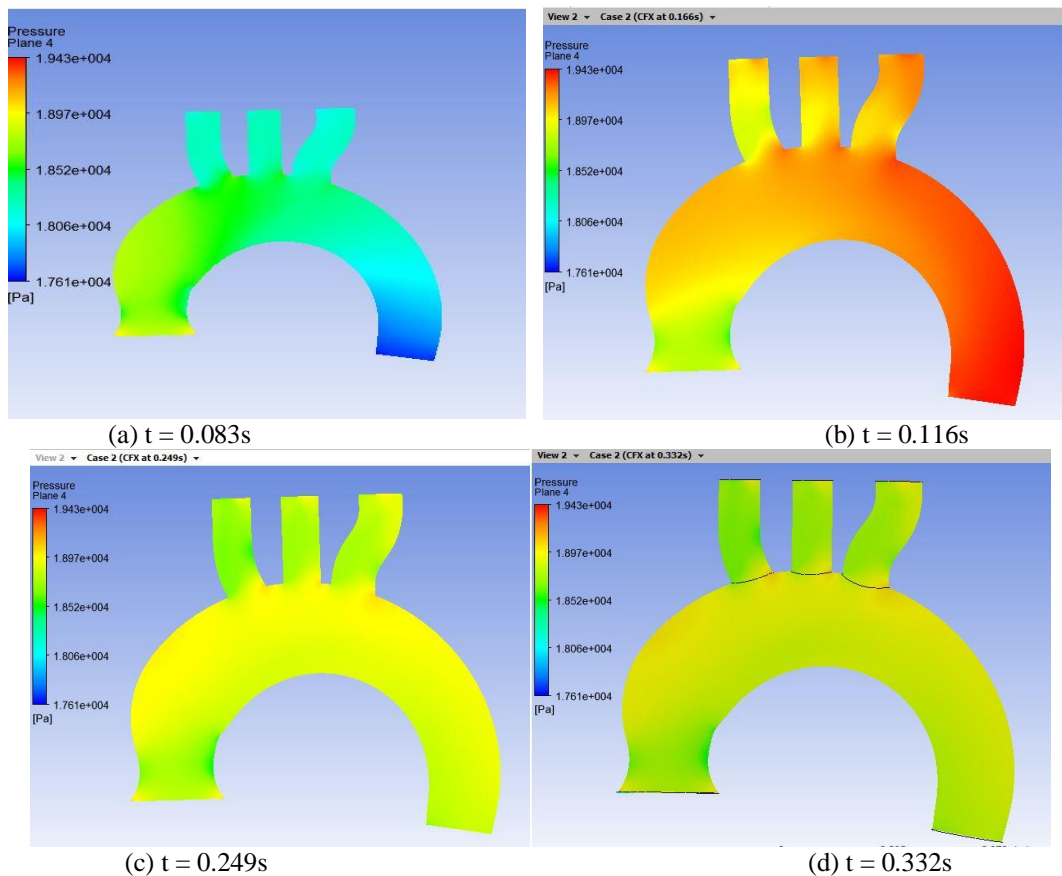


(i) $t = 0.747s$

(j) $t = 0.83s$

Fig.6 (Continued)

2. Pressure Contours



(a) $t = 0.083s$

(b) $t = 0.116s$

(c) $t = 0.249s$

(d) $t = 0.332s$

Fig.7 Pressure variation at each time step

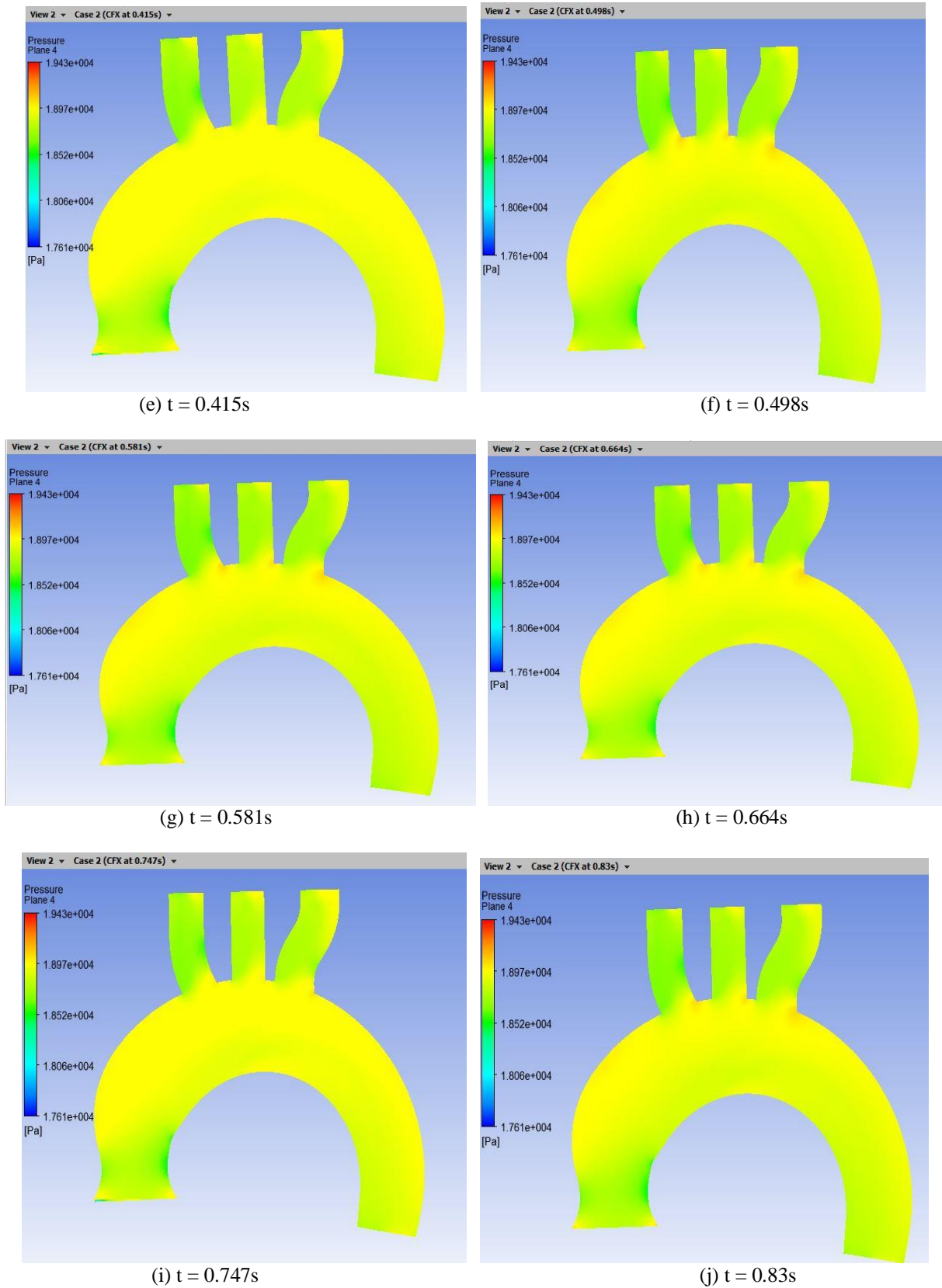


Fig.7 (Continued)

Fig 7 shows that, in some portion of descending aorta pressure is minimum at 0.083 seconds and it is maximum at 0.116 seconds. As the flow accelerates pressure is gradually decreases in the branches of aorta. At the root of brachiocephalic and subclavian arteries pressure is found to be maximum shown in Fig 8 (a) and (b). In the inner and outer curvature of aorta pressure variation is approximately uniform during the flow deceleration phase.

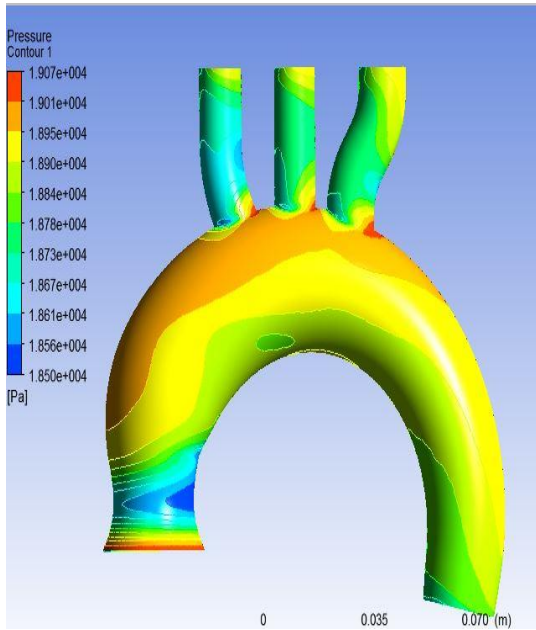


Fig.8 Pressure contour (a)

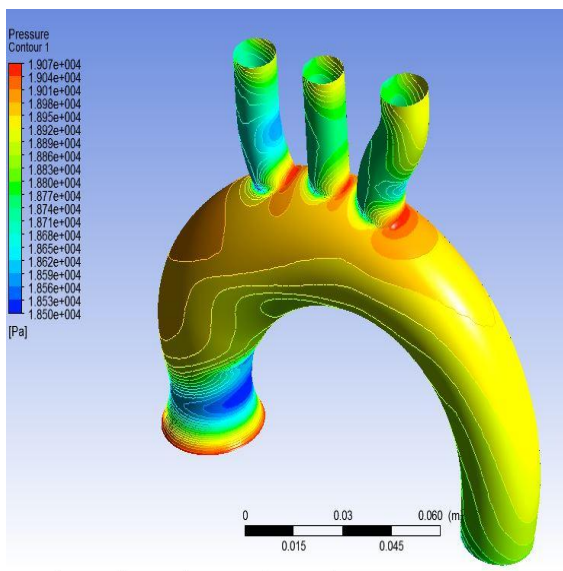


Fig.8 Pressure contour (b)

3. Total Mesh Displacement

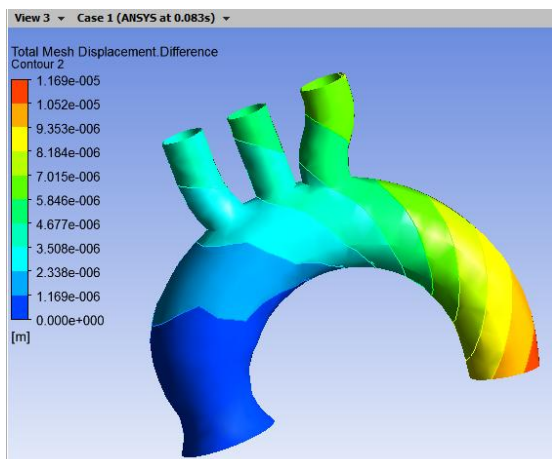


Fig. 9 Total mesh displacement contour

In Fig 9 Total mesh displacement contour has been plotted, it is observed that Total mesh displacement is maximum at 0.083 s i.e. at the start of stroke. Total mesh displacement increases as velocity and obstruction to the flow increases in the region of the brachiocephalic, subclavian artery and at the end portion of descending Aorta. Total mesh displacement of fluid with respect to structure is varies maximum within the range of 6% shown in Fig 10.

V. MODEL VALIDATION

To prove the validation of the model is to compare the CFD results with similar ones in previous publications or experimental data. The comparisons between the simulation results from this study and similar ones in previous publications were performed. Velocity flow pattern of the Aorta is shown in Fig. 6. High velocities are clearly observed at right curvature of BCA, LCCA and LSA Similar kind of the flow was also found by A.C Benin et al. in fig.4 of detailed plot of velocity magnitude [10] which verifies this study.

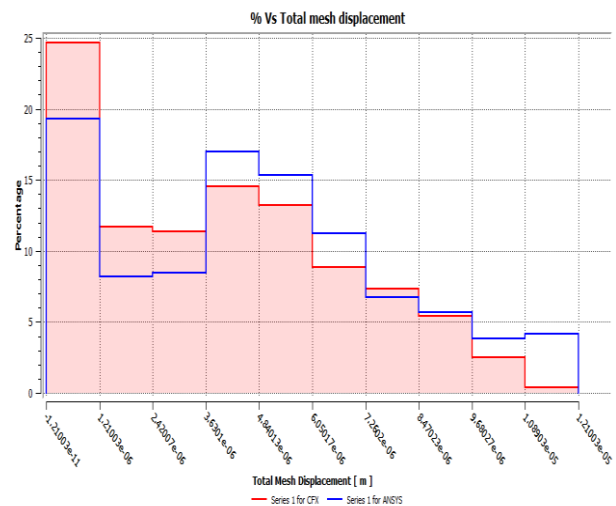


Fig 10 Total Mesh Displacement of fluid with respect to Structure

VI. CONCLUSION

In this work, blood flow behaviour of aorta subject to pre high blood pressure and normal velocity were modeled employing fluid structure interaction method. The effect of blood pressure and blood velocity on flow structure of aorta wall was studied in detail. Some limitations should be mentioned in this work. The model used in this study was an geometrically created model. However, in reality, aorta model is somewhat complex as compared to created geometry in CATIA V5. These factors will be considered in future researches on geometry of aorta. Besides, the gravity effect on the fluid and structure regions of the model may be important when considering this model in clinical applications. It is clear that from the results obtained from this analysis and the relevant findings of previous authors that the view is very positive. It is thought that with the continued achievement of clinical

validation trials and the constantly refining computer technology, the accurate prediction of blood flow behaviour of aorta will be captured. Clinical management of heart patient will be improved in the near future.

REFERENCES

- [1] Jin Suo, investigation of blood flow patterns and hemodynamics in the human ascending aorta and major trunks of right and left coronary arteries using magnetic resonance imaging and computational fluid dynamics, January 2005
- [2] Office of research on women's health, Women of Color Health Information Collection Cardiovascular Disease.
- [3] Larissa Huetter*, et al Application of a meta-analysis of aortic geometry to the generation of a compliant phantom for use in particle image velocimetry experimentation, 2405-8963 © 2015, IFAC (International Federation of Automatic Control) Hosting by Elsevier Ltd.
- [4] Mona Alimohammadi1, et al Aortic dissection simulation models for clinical support: fluid-structure interaction vs. rigid wall models BioMedical Engineering OnLine (2015)
- [5] M. Malvè, et.al, Unsteady blood flow and mass transfer of a human left coronary artery bifurcation: FSI vs. CFD, International Communications in Heat and Mass Transfer 39 (2012) 745–75, 2012
- [6] M. Alishahi, M.M. Alishahi *, H. Emdad, Numerical simulation of blood flow in a flexible stenosed abdominal real aorta, accepted 20 September 2011
- [7] Tina M. Morrison, PhD Circumferential and Longitudinal Cyclic strain of the human thoracic Aorta; Age related changes, Journal of vascular surgery, April 2009
- [8] Patric Biaggi, Gender, Age, and Body Surface Area are the Major Determinants of Ascending Aorta Dimensions in Subjects With Apparently Normal Echocardiograms, Journal of the American Society of Echocardiography Volume 22 Number 6, 2009
- [9] Xiaohong wang, et al Computational simulation of aortic aneurysm using FSI method; Influence of blood viscosity on aneurysmal dynamic behaviours. © 2011 Elsevier Ltd.
- [10] P. Causin, J.F. Gerbeau, and F. Nobile. Added-mass effect in the design of partitioned algorithms for fluid-structure problems. Comput. Methods Appl. Mech. Engrg., 94(42-44):4506–4527, 2005.
- [11] Redheuil A., Yu W.-C., Mousseaux E., Harouni A.A., Kachenoura N., Wu C.O., Bluemke D., Lima J.A.C. (2011) Age-Related Changes in Aortic Arch Geometry: Relationship with Proximal Aortic Function and Left Ventricular Mass and Remodeling, Journal of the American College of Cardiology, 58(12), 1262-1270
- [12] Giuseppe Mancia (Chairperson) (Italy); et.al The Task Force for the management of arterial hypertension of the European Society of Hypertension (ESH) and of the European Society of Cardiology (ESC) Journal of Hypertension 2013, 31:1281–1357
- [13] Takayoshi Fukushima et.al; Numerical Analysis of Blood Flow in the Vertebral Artery, Journal of Biomechanical Engineering MAY 1982, Vol. 104/143
- [14] C. A. Kouser, N. B. Wood et.al, A Numerical Study of Aortic Flow Stability and Comparison With In Vivo Flow Measurements, Journal of Biomechanical Engineering, January 2013, Volume 135